Journal of Applied Mechanics and Technical Physics, Vol. 47, No. 3, pp. 394–400, 2006

PLANE STRAIN WAVE IN AN ISOTROPIC LAYER OF A VISCOELASTIC MATERIAL

V. M. Kulik

UDC 532.591; 539.3.371

The velocity and the rate of decay of a strain wave in a layer of a viscoelastic material rigidly fixed on a solid foundation are determined. The wave structure (ratio of the longitudinal to the transverse displacement) and the profiles of these displacements are analyzed. Attenuation of waves in the first mode is found to be more significant than that in an infinite space. The most intense decay is observed at resonance frequencies. A strong effect of compressibility of the medium on wave parameters is revealed. Conditions at which such a system operates as a waveguide are found. For a loss tangent higher than 0.13 *(for an incompressible medium), the character of the dispersion dependence is observed to change drastically: the wave velocity decreases with decreasing frequency.*

Key words: *viscoelastic material, wave velocity, decay, profile, longitudinal and transverse displacements.*

The velocity of free oscillations propagating in a layer of a viscoelastic material of thickness H with elasticity modulus E, density ρ, Poisson's ratio σ, and loss tangent μ is calculated in the present paper.

Let us consider a plane monochromatic wave propagating along the x axis. The displacement of particles of the medium in this wave is

$$\boldsymbol{\xi} = \boldsymbol{i}\zeta + \boldsymbol{j}\eta = \boldsymbol{f}(y)\,\mathrm{e}^{ik(x-Vt)},$$

where ζ and η are the displacement components directed along the coating and perpendicular to it, respectively.

The general equation of motion has the form [1]

$$\frac{\partial^2 \boldsymbol{\xi}}{\partial t^2} = C_t^2 \Delta \boldsymbol{\xi} + (C_l^2 - C_t^2)\,\mathrm{grad}\,\mathrm{div}\,\boldsymbol{\xi}, \tag{1}$$

where $C_l = [E(1-\sigma)/(\rho(1+\sigma)(1-2\sigma))]^{1/2}$ is the velocity of propagation of a compression-extension wave in which the displacement is parallel to the wave direction and $C_t = [E/(2\rho(1+\sigma))]^{1/2}$ is the velocity of propagation of a shear wave where the displacement is perpendicular to the wave direction, both waves propagating in an infinite space.

The boundary conditions are the absence of displacements on the solid wall

$$\zeta = \eta = 0 \qquad \text{for} \quad y = H \tag{2}$$

and the absence of stresses on the outer boundary

$$C_l^2 \frac{\partial \eta}{\partial y} + (C_l^2 - 2C_t^2)\,\frac{\partial \zeta}{\partial x} = 0, \qquad \frac{\partial \zeta}{\partial y} + \frac{\partial \eta}{\partial x} = 0 \qquad \text{for} \quad y = 0. \tag{3}$$

As in the Rayleigh wave [2], the displacement is determined as a sum of the longitudinal and transverse waves. By virtue of the boundary conditions, the longitudinal wave is not parallel to the x axis and the transverse wave is not perpendicular to it.

Kutateladze Institute of Thermophysics, Siberian Division, Russian Academy of Sciences, Novosibirsk 630090; kulik@itp.nsc.ru. Translated from Prikladnaya Mekhanika i Tekhnicheskaya Fizika, Vol. 47, No. 3, pp. 104–111, May–June, 2006. Original article submitted February 9, 2005; revision submitted August 1, 2005.

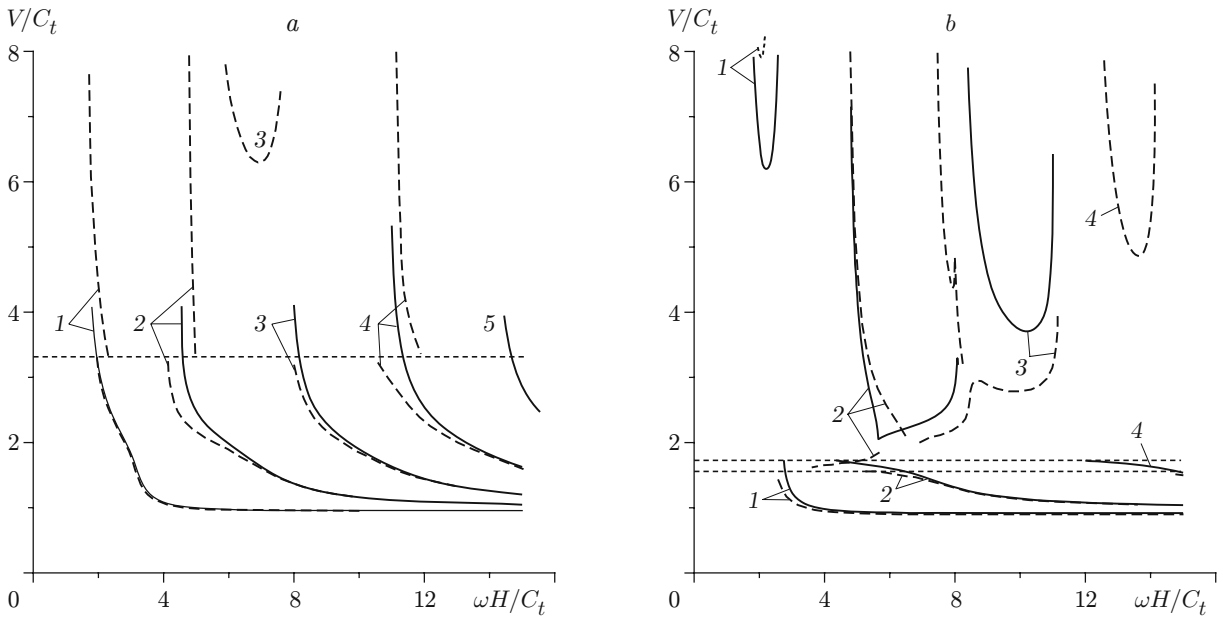

Fig. 1. Dispersion of the wave velocity for different Poisson's ratios: (a) $\sigma = 0.45$ (dashed curves) and 0.50 (solid curves); (b) $\sigma = 0.15$ (dashed curves) and 0.25 (solid curves); the dotted curves refer to $V/C_t = \sqrt{2(1-\sigma)/(1-2\sigma)}$; the numbers of oscillation modes are indicated by 1–5.

To solve Eq. (1), we use the method of displacement division into the gradient and rotor components. We introduce two scalar functions Φ and Ψ such that

$$\zeta = \frac{\partial \Phi}{\partial x} + \frac{\partial \Psi}{\partial y}, \qquad \eta = \frac{\partial \Phi}{\partial y} - \frac{\partial \Psi}{\partial x}.$$

Substituting them into Eq. (1), we obtain the equations

$$\frac{\partial^2 \Phi}{\partial t^2} - C_l^2 \Delta \Phi = 0, \qquad \frac{\partial^2 \Psi}{\partial t^2} - C_t^2 \Delta \Psi = 0,$$

whose solution has the form

$$\Phi = \left[A_1 \frac{\sinh(\alpha k y)}{\alpha k} + B_1 \cosh(\alpha k y)\right] e^{ik(x-Vt)}, \qquad \Psi = \left[A_2 \frac{\sinh(\beta k y)}{\beta k} + B_2 \cosh(\beta k y)\right] e^{ik(x-Vt)}.$$

Here $\alpha = [1-(V/C_l)^2]^{1/2}$ and $\beta = [1-(V/C_t)^2]^{1/2}$.

Using the boundary conditions (2) and (3), we obtain a homogeneous system of four equations for A_1, A_2, B_1, and B_2. As the determinant of this system equals zero, we have the characteristic equation for the velocity of oscillations

$$[2-(V/C_t)^2]^2[\cosh(\alpha k H)\cosh(\beta k H) - (\alpha\beta)^{-1}\sinh(\alpha k H)\sinh(\beta k H)]$$

$$+ 4[\cosh(\alpha k H)\cosh(\beta k H) - \alpha\beta\sinh(\alpha k H)\sinh(\beta k H)] = 4[2-(V/C_t)^2]. \qquad (4)$$

As $H \to \infty$, this equation transforms to the conventional equation for Rayleigh waves [1, 2], which are shear waves propagating along the interface between two media.

As

$$\alpha^2 = 1 - \left(\frac{V}{C_t}\right)^2 \left(\frac{C_t}{C_l}\right)^2 = 1 - \left(\frac{V}{C_t}\right)^2 \frac{1-2\sigma}{2(1-\sigma)},$$

and the arguments of hyperbolic functions are proportional to $kH = 2\pi H/\lambda = (\omega H/C_t)/(V/C_t)$, then V/C_t and $\omega H/C_t$ are modeling parameters, which were the sought variables in Eq. (4). The solution of this equation for an ideal material [incompressible ($\sigma = 0.5$) and devoid of viscous losses ($\mu = 0$)] was obtained in [3].

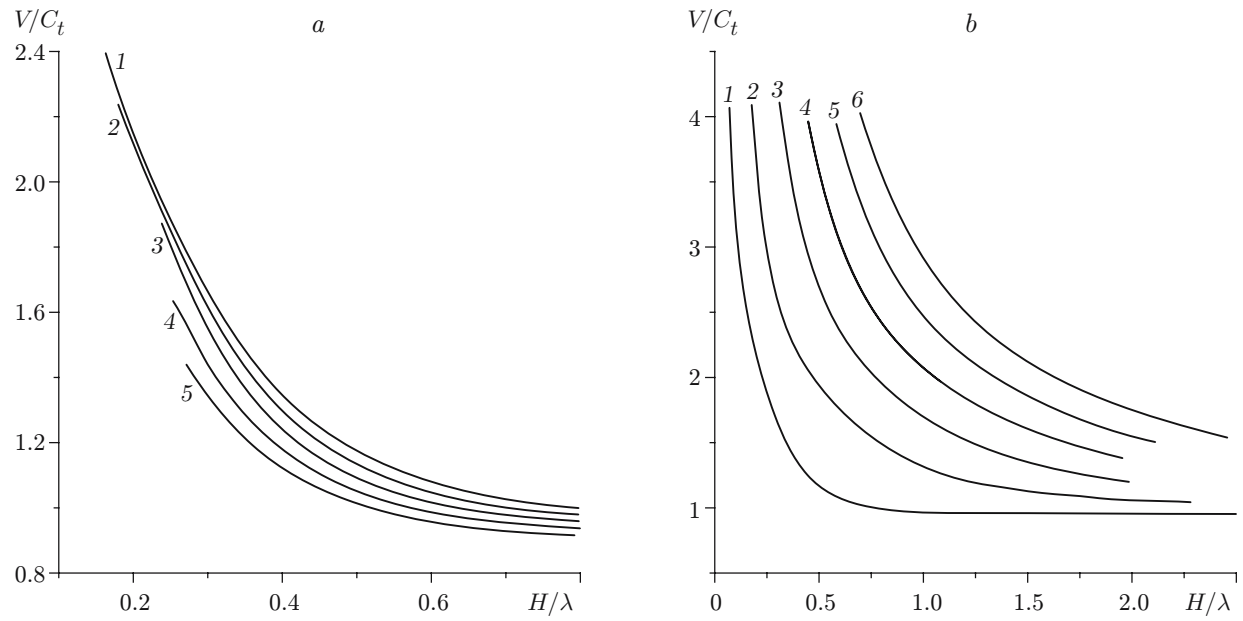

Fig. 2. Low-velocity portions of the dispersion curves: (a) first mode of oscillations with $\sigma = 0.5$ (1), 0.4 (2), 0.3 (3), 0.2 (4), and 0.1 (5); (b) different modes of oscillations with $\sigma = 0.5$ (the numbers of oscillation modes are indicated by 1–6).

Figure 1 shows the results of solving Eq. (4) with different values of Poisson's ratio. For each mode, the dispersion curve has three characteristic portions corresponding to the Rayleigh waves with $\omega H/C_t \gg 1$ ($V/C_t < 1$), the transitional zone with $1 < V/C_t < [2(1-\sigma)/(1-2\sigma)]^{1/2}$ (portions located below the dotted curves in Fig. 1), and the long-wave zone (portions located above the dotted curves in Fig. 1).

For $\sigma = 0.5$ (solid curves in Fig. 1a), the long-wave zone is absent. The first mode of oscillations has the least velocity of propagation at a fixed frequency. For $\omega H/C_t \leqslant 1.8$, the strain-wave velocity drastically increases, and we can assume that oscillations in the coating are impossible if $\omega H/C_t < 1.5$. As the oscillation frequency increases, higher and higher modes with a periodicity interval $\omega H/C_t \approx 4.45$ appear. This happens because β is an imaginary quantity; hence, sinh β and cosh β are conventional harmonic functions.

For real materials, which have a certain compressibility, the situation is more complicated. Thus, for $\sigma = 0.45$ (dashed curves in Fig. 1a), the dispersion curves for the first, second, and fourth modes pass to the region above the dotted curve: the curves experience a discontinuity and are shifted to the right. The upper part of the dispersion curve corresponding to the third mode has a parabolic shape and is located above the discontinuity curve. The curves below the dotted curve are not rigorously periodic, in contrast to the solid curves.

As Poisson's ratio decreases, the interface between the zones is shifted downward (from $V/C_t = 3.316$ for $\sigma = 0.45$ to $V/C_t = 1.5$ for $\sigma = 0.15$). The upper parts of the dispersion curves are parabolic or have a more complicated shape (e.g., solid curve 2 in Fig. 1b). For $\sigma = 0.15$, it is already impossible to determine which mode the curves above the dotted curve correspond to.

Of the greatest interest for applications is the study of the first mode of oscillations [4]. In experiments, the coating is normally characterized either by measured viscoelastic properties of its material (elasticity modulus and loss tangent as functions of frequency [5]) or by oscillatory characteristics of the coating itself (velocity of disturbances and their decay [6]). In the latter case, the data can be reasonably presented as the dependence of V/C_t on the dimensionless parameter H/λ, which has a physical meaning.

Figure 2a shows the dependence of V/C_t on H/λ for the transitional zone of the dispersion dependence of the first mode of oscillations. As the medium compressibility increases (σ decreases), the dimensionless velocity of the wave V/C_t decreases. The curves are bounded from above by the limiting values

$$\frac{V}{C_t} = \sqrt{\frac{2(1-\sigma)}{1-2\sigma}}$$

and reach the Rayleigh asymptotic value $V/C_t \approx 0.141\sigma + 0.885$ as $H/\lambda \to \infty$ (for $\sigma > 0.3$).

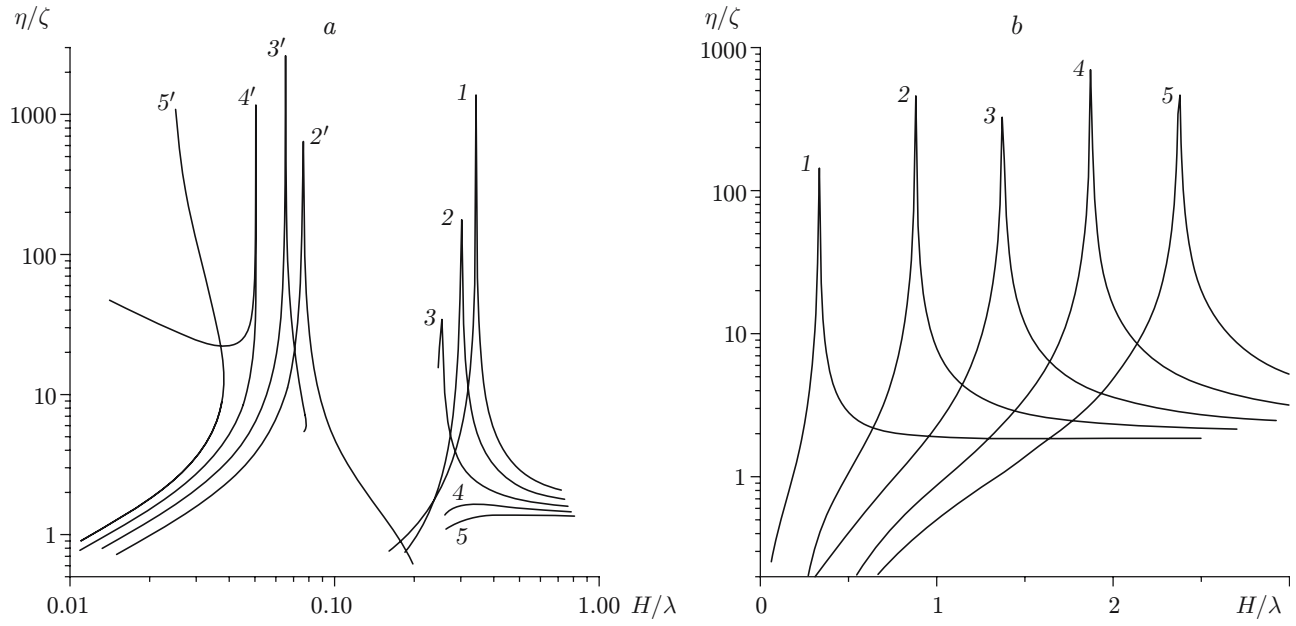

Fig. 3. Ratio of the vertical to the horizontal displacement at the outer boundary of the layer: (a) first mode with $\sigma = 0.5$ (1), 0.4 (2 and 2′), 0.3 (3 and 3′), 0.2 (4, and 4′), and 0.1 (5 and 5′); curves 1–5 show the low-velocity portions of the dispersion curves in Fig. 1; curves 2′–5′ show the high-velocity portions of the dispersion curves in Fig. 1; (b) different modes with $\sigma = 0.5$ (the numbers of oscillation modes are indicated by 1–5).

Figure 2b shows the dispersion of velocity of the strain wave for the first six modes of oscillations for $\sigma = 0.5$.

Figure 3a shows the ratio of the vertical to the horizontal displacement at the outer boundary of the layer for different Poisson's ratios. The first mode has two maximums (curves 1–3 for the portions of the dispersion curves located below the dotted curve in Fig. 1 and curves 2′–5′ for the portions of the dispersion curves located above the dotted curve in Fig. 1) corresponding to the resonance frequencies of the amplitude of surface bending. The vertical displacement is ahead of the horizontal one by a phase angle equal to 90° changing to 180° as the resonance point is passed. The resonance for low-velocity waves (curves 1–5 in Fig. 3a) is reached for some values of σ only. As Poisson's ratio decreases, the resonance frequency decreases following the dependence

$$f_0 \simeq C_t(\sigma + 1.11)/(\pi H)$$

to values corresponding to the discontinuity line; therefore, curves 4 and 5 ($\sigma = 0.2$ and 0.1, respectively) have no resonance peak. The resonances for high velocities of strain waves (curves 2′–5′ in Fig. 3a) correspond to the interval $0.25 < H/\lambda < 0.75$. The resonance frequency of the high-velocity portion of the dispersion curve of the first mode drastically increases with decreasing σ, and multiple-valuedness is observed for $\sigma < 0.2$: two values of η/ζ are possible for one value of H/λ.

For $H/\lambda \gg 1$, the relation for the Rayleigh waves is valid:

$$\frac{\eta}{\zeta} = i\,\frac{2 - (V/C_t)^2}{2\sqrt{1 - (V/C_t)^2}}.$$

Figure 3b shows the ratio of the vertical to the horizontal displacement at the outer boundary of the layer for the low-velocity portion of the dispersion curves of different modes with $\sigma = 0.5$. The first resonance is observed for $H/\lambda \simeq 0.333$, and then the resonances follow equidistantly with $H/\lambda \approx 0.5$.

The profiles of the vertical and horizontal displacements are responsible for the strain-wave structure. Figure 4 shows the distribution of displacements over the coating thickness for the first three modes of oscillations with $\sigma = 0.5$. The curves are shown only for the resonance frequencies of the corresponding modes. The displacements on the solid wall are equal to zero for all modes of oscillations. The vertical displacement at the resonance frequency of the first mode of oscillations (curve 1 in Fig. 4a) smoothly increases over the coating thickness and reaches a

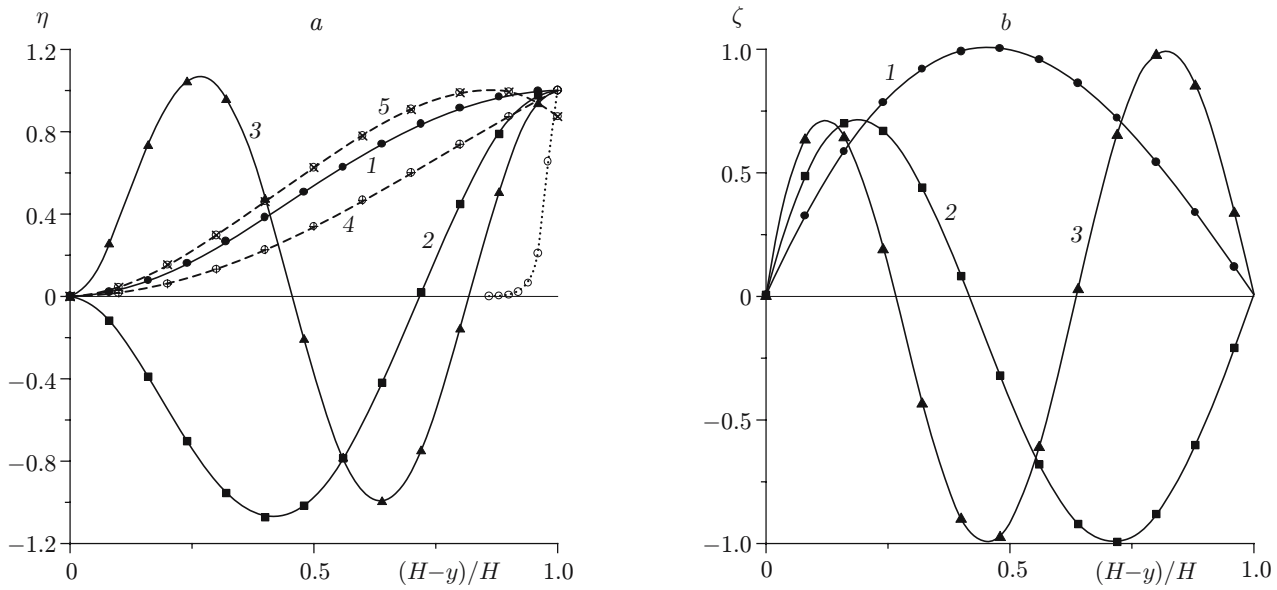

Fig. 4. Profiles of the vertical (a) and horizontal (b) displacements with $\sigma = 0.5$: the solid curves are the resonance frequencies of different modes (the numbers of modes are indicated by 1–3); the dashed curves are the frequencies multiple to the resonance frequency of the first mode [$H/\lambda = 0.17$ (4) and 0.66 (5)]; the dotted curve refers to $H/\lambda = 30$ (Rayleigh wave).

maximum at the outer boundary. The second mode (curve 2) consists of a "negative" half-wave [the displacement is out of phase for $0 < (H - y)/H < 0.7$] and 1/4 of the length of the wave with "positive" strains. The maximum strain observed for $(H - y)/H \approx 0.42$ is 7.5% higher than the strain on the outer wall. The third mode is 5/4 of the oscillation period, the fourth mode is 7/4 of the oscillation period, and each next mode has 1/2 of the oscillation period more.

The profile of the horizontal displacement of the first mode of oscillations (curve 1 in Fig. 4b) is a half-wave with zero displacements on the outer and inner boundaries. The maximum displacement is observed for $(H - y)/H = 0.46$. The second mode (curve 2) corresponds to one period of oscillations, the amplitude of the "positive" wave being lower than that of the "negative" wave by a factor of $\sqrt{2}$. Half of the oscillation period is added to each next mode.

For frequencies other than the resonance frequency, the profiles of displacements for the first mode of oscillations with $\sigma = 0.5$ are plotted by the dashed curves in Fig. 4a. For a frequency twice lower than the resonance frequency (curve 4 in Fig. 4a), the vertical displacement profile is almost linear for $(H - y)/H > 0.5$. After the transition through the resonance point (at $H/\lambda > 0.33$), the maximum displacement is reached at a certain distance from the outer surface (curve 5). The logarithmic profile typical of the Rayleigh waves is reached only for rather high values of H/λ (curve 6 corresponding to $H/\lambda = 30$). The dependences plotted in Fig. 4 cannot be compared in absolute values because the curves are normalized by different coefficients.

For a plane traveling wave $\xi = \xi_0 \, \mathrm{e}^{i\omega(t-x/V)}$ propagating in an infinite space filled by a viscoelastic material with a dynamic elasticity modulus $\hat{E} = E(1 + i\mu)$, the wave velocity is determined by the formula

$$V = \sqrt{\frac{E}{\rho}} \, \frac{\sqrt{\sqrt{1+\mu^2}+1} + i\sqrt{\sqrt{1+\mu^2}-1}}{\sqrt{2}}.$$

The viscous losses lead to a change in the wave length and its decay:

$$\zeta = \zeta_0 \exp\Big[i\omega\Big(t - \frac{x}{\sqrt{E/\rho}}\sqrt{\frac{\sqrt{1+\mu^2}+1}{2(1+\mu^2)}}\,\Big)\Big] \exp\Big(-2\pi\,\frac{x}{\lambda}\sqrt{\frac{\sqrt{1+\mu^2}-1}{\sqrt{1+\mu^2}+1}}\,\Big). \tag{5}$$

For $\mu < 0.1$, we have $\lambda = \lambda_0\sqrt{2(1+\mu^2)/(\sqrt{1+\mu^2}+1)} \approx \lambda_0(1 + 3\mu^2/8)$. The decay parameter L, i.e., the distance x at which the wave amplitude decreases by a factor of e is calculated as

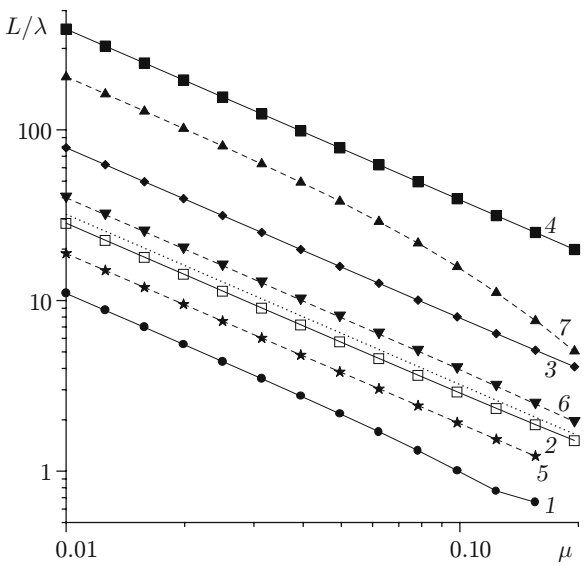

Fig. 5

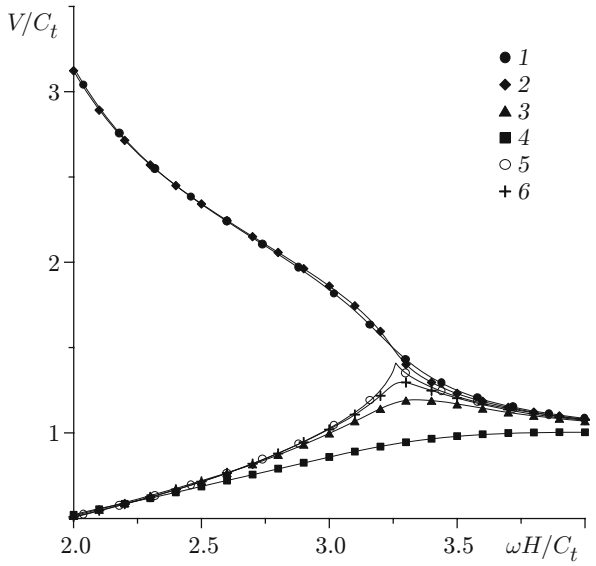

Fig. 6

Fig. 5. Decay parameter of the wave versus the loss coefficient for $\sigma = 0.5$: the solid curves refer to the low-velocity portion of the dispersion curve of the first mode [f_0 (1), $f_0/2$ (2), $2f_0$ (3), and $3f_0$ (4)]; the dashed curves refer to the high-velocity portion of the dispersion curve of the first mode at resonance frequencies [$\sigma = 0.4$ (5), 0.3 (6), and 0.25 (7)]; the dotted curve refers to the sonic wave in an infinite space [see Eq. (5)].

Fig. 6. Wave velocity versus frequency for $\sigma = 0.5$ and $\mu = 0.01$ (1), 0.1 (2), 0.2 (3), 0.4 (4), 0.13 (5), and 0.15 (6).

$$L = \frac{\lambda}{2\pi}\sqrt{\frac{\sqrt{1+\mu^2}+1}{\sqrt{1+\mu^2}-1}}.$$

For $\mu < 0.1$, we have $L \approx \lambda/(\pi\mu)$.

A similar pattern is observed in a layer of a viscoelastic material. Figure 5 shows the decay parameter

$$\frac{L}{\lambda} = \frac{1}{2\pi}\,\frac{\mathrm{Re}\,(V/C_t)}{\mathrm{Im}\,(V/C_t)}$$

as a function of the loss tangent μ for the first mode of oscillations. The maximum decay is observed at the resonance frequency. With distance from the resonance point, the decay becomes much less intense than the decay of acoustic waves in this medium (dotted curve in Fig. 5). The decay becomes more intense with increasing loss tangent, and the amplitude decreases by a factor of e at a distance equal to the wave length for $\mu = 0.1$.

The dashed curves in Fig. 5 show the decay length of the high-velocity portion of the dispersion curve of the first mode at resonance frequencies (frequencies corresponding to the maximums of curves $2'$–$4'$ in Fig. 3a). As for the low-velocity portion of the dispersion dependence, the maximum decay is reached for an incompressible materials, whereas the ratio L/λ increases with increasing σ. In this case, the wave length is much greater than the coating thickness, and such a system operates as a waveguide, i.e., it transfers disturbances without decay to large distances.

Figure 6 shows the wave velocity as a function of frequency for the loss tangent varied in a wide range. The nonlinear character of Eq. (4) with respect to μ is manifested in the existence of two branches of the dispersion dependence of wave velocity. The value $\mu = 0.13$ is the branching point for $\sigma = 0.5$ (the critical value of μ decreases with decreasing Poisson's ratio). The existence of the low-velocity branch of the dispersion dependence of strain velocity makes it possible to create compliant coatings for decreasing the friction drag in the range of velocities used in practice and disproves the conclusion made in [3] on the lack of prospects of single-layer monolithic coatings.

The conclusions drawn in the present paper need experimental verification with the use of the technique proposed in [6].

REFERENCES

1. L. D. Landau and E. M. Lifshitz, *Theory of Elasticity*, Pergamon Press, Oxford (1986).
2. L. Rayleigh, "On waves propagated along the plane surface of an elastic solid," *Proc. London Math. Soc.*, **17**, 4–11 (1885).
3. M. Gad-el-Hak, R. F. Blackwelder, and J. J. Riley, "On the interaction of compliant coatings with boundary layer flows," *J. Fluid Mech.*, **140**, 257–280 (1984).
4. V. M. Kulik, S. V. Rodaykin, T. Lee, and H. H. Chun, "Deformation of a viscoelastic coating under the action of convective pressure fluctuations," *Exp. Fluids*, **38**, No. 5, 648–655 (2005).
5. V. M. Kulik and B. N. Semenov, "Two-parameter method of measuring viscoelastic properties of polymer materials," *Metrologiya*, No. 4, 32–38 (1986).
6. V. M. Kulik, "Propagation of strain waves in a compliant coating," *Inzh.-Fiz. Zh.*, **77**, No. 4, 71–75 (2004).